Comparison of four mobility particle sizers with different time resolution for stationary exposure measurements

Christof Asbach[1], Heinz Kaminski[1], Heinz Fissan[1], Christian Monz[2], Dirk Dahmann[2], Sonja Mülhopt[3], Hanns R. Paur [3], Heinz J. Kiesling[4], Friedhelm Herrmann[4], Matthias Voetz[4], Thomas A.J. Kuhlbusch[1]

[1] Institut für Energie- und Umwelttechnik (IUTA), 47229 Duisburg, Germany
[2] Institut für Gefahrstoffforschung (IGF), 44789 Bochum, Germany
[3] Forschungszentrum Karlsruhe, 76344 Eggenstein-Leopoldshafen, Germany
[4] Bayer Technology Services GmbH, 51368 Leverkusen, Germany

Abstract

Exposure to airborne ultrafine and nanoparticles has raised increased interest over the recent years as they may cause adverse heath effects. A common way to quantify exposure to airborne particles is to measure particle number size distributions through electrical mobility analysis. Four mobility particle sizers have been subject to a detailed intercomparison study, a TSI FMPS, a Grimm SMPS+C and two TSI SMPS's, equipped with two different CPC's. The instruments were challenged with either NaCl or Diesel soot particles. The results indicate that the sizing of all tested instrument was similar with only the FMPS size distributions consistently shifted towards smaller particle sizes. The Grimm SMPS generally measured higher concentrations and broader distributions than the TSI instruments. The two Grimm DMA's agreed well with each other, however, the TSI SMPS results showed a reproducible dependence the flow rates. While TSI and Grimm SMPS's delivered consistent results for NaCl and Diesel soot, the FMPS seemed to react differently to the changing particle source than the SMPS's, which may be caused by either the different morphology or particle size dependent effects. For NaCl particles, the FMPS delivered the narrowest distributions and concentrations comparable with TSI SMPS's, whereas for Diesel soot, it delivered the broadest distributions and higher concentrations than TSI SMPS's.

Introduction

Several studies have shown that health effects may arise from the inhalation of small particles (Atkinson *et al.*, 2001; Dockery *et al.*, 1993; Donaldson *et al.*, 1998; Kreyling *et al.*, 2002; Oberdörster *et al.*, 2004; Oberdörster, 2000). The risk of such particles is a function of their potential hazard and the exposure thereto. Exposure to such particles therefore needs to be assessed. Particles with equivalent diameters below

100 nm are generally distinguished into intentionally produced nanoparticles and ubiquitous ultrafine particles. For simplicity, all particles with diameters ≤ 100 nm will be referred to as nanoparticles (NPs) in this paper, independent of their source.

Current legislative limits for ambient or workplace airborne particle concentrations are based on the integral particle mass concentration of all particles below a certain size. The size limits are 10 µm (PM_{10}) or 2.5 µm ($PM_{2.5}$) for ambient air, and e.g. 4 µm (PM_4) for workplaces. However, NPs have only very small masses and therefore generally contribute negligibly to these integral mass concentrations. More NP-sensitive techniques are therefore required to detect those particles in air. Unlike the particle mass, which is weighted with the particle diameter to the third power, the particle number is unweighted and therefore the most sensitive measure for NP concentrations. Peters *et al.* (1997) also suggested that respiratory effects are directly associated with the number of ultrafine particles. The most widely spread method to determine airborne particle number concentrations as a function of particle size, i.e. particle number size distributions, is based on electrical mobility analysis of the particles. Exposure measurements may face aerosols that can be everything from quickly changing to stable over longer time depending on processes and activities in the vicinity of the measurement location. Time resolution may therefore play a crucial role when choosing an appropriate mobility particle sizer, besides its accuracy and size resolution. The time resolution of the tested instruments was 1 s in case of the FMPS and on the order of several minutes for all SMPS's.

Besides control equipment and evaluation software, these techniques usually comprise three main components: (1) a particle charger to predictably charge particles depending on their size; (2) a mobility analyzer which classifies the particles of one polarity according to their electrical mobility; and (3) a particle counter that determines the number concentration of the mobility-classified particles. These mobility particle sizers are available from different manufacturers and in various designs for different size class resolutions and overall size ranges. These instruments are usually calibrated by the manufacturers only for spherical particles (Kinney *et al.,* 1991; Mulholland *et al.*, 2006). Although attempts have been made to produce reference particle number concentrations (Koch et al., 2008), as of now no standard method has been agreed upon for the provision of reference number concentrations. Each instrument may therefore react differently not only to changing particle concentrations, but also to different morphologies and materials. In exposure

studies, the knowledge of potentially different results from different instruments is essential when results obtained simultaneously at two different locations are to be compared. This is particularly important when a reference site is required besides the workplace measurement site in order to distinguish ubiquitous particles from particle emitted in the workplace (Kuhlbusch *et al*., 2004, 2006, 2009). In the study presented here, three different mobility particle sizer models from two manufacturers were compared with each other, namely a Fast Mobility Particle Sizer Spectrometer (FMPS model 3091; TSI, Shoreview, MN, USA), a Scanning Mobility Particle Sizer (SMPS model 3080, TSI, Shoreview, MN, USA), and a Sequential Mobility Particle Sizer (SMPS+C, Grimm Aerosol Technik GmbH & Co. KG, Ainring, Germany). The FMPS measured all covered particle sizes simultaneously with a time resolution of 1 s. TSI SMPS's were both operated with a long-column DMA (TSI, model 3081) and set to sample at a time resolution of 300 s (240 s scan time, 20 s retrace and 40 s wait). The default total scan time of the Grimm SMPS was 230 s when operated with the short DMA (Grimm Aerosol Technik, model M-DMA) and 406 s when operated with the long DMA (Grimm Aerosol Technik, model L-DMA). Two identical handheld condensation particle counters (CPC model 3007, TSI, Shoreview, MN, USA) simultaneously sampled from the same source. Handheld CPC's are commonly used in industrial hygiene for quick measurements or mapping of particle number concentrations. A list of all instruments tested is given in Table 1. All instruments were simultaneously challenged with the same aerosol, containing either sodium chloride (NaCl) or Diesel soot. These particle sources were chosen because they can exhibit very different morphologies. While NaCl usually forms cubic or (near-) spherical particles, Diesel soot is known to appear in the shape of agglomerates which may be covered with hydrocarbon compounds and can exhibit a wide range of fractal dimensions, depending on type and load of the Diesel engine (Harris and Maricq, 2001; Park et al., 2003).

Experimental

Experiments were conducted using an approximately 20 m long, cylindrical wind tunnel with a diameter of 0.7 m, connected to a 20 m³ exposure chamber, located at the facilities of the Institut für Gefahrstoffforschung (IGF) in Dortmund, Germany. The experimental set up is shown in Figure 1. The same facilities were used for an earlier comparison of mobility particle sizers by Dahmann *et al*. (2001). In their study, they compared eleven different mobility particle sizers, ten out of them were different

models of a TSI-SMPS. Only soot particles at different concentration levels from either the same Diesel engine as in this study or from a quenched flame soot generator were used as test aerosol. Helsper *et al*. (2008) recently published a comparison study of five mobility particle sizers (2x Grimm SMPS with M-DMA, 2x TSI SMPS with long and Nano-DMA, respectively, and 1x custom made TDMPS). They sampled ambient air directly from a street canyon in Leipzig and smoothed possible quick fluctuations of the size distributions by passing the aerosol through a 20 liter buffer volume. The time resolution of the instruments in their test was between four and nine minutes. The study presented here employed SMPS's from two manufacturers plus a completely different instrument (FMPS) with very high time resolution of 1 s that has not been subject to such an intense investigation before. Furthermore the particle sizers were challenged with defined particle materials and morphologies to study their effect on the instruments' response, whereas the aforementioned previous studies concentrated on a single type of aerosol, soot or ambient.

Particle generators were connected to the wind tunnel at the opposite end of the exposure chamber. Particle free dilution air with controllable flow rate was added to the test aerosol. The long wind tunnel allowed for a homogenous mixing of the particles with dilution air. The concentrations were measured across the cross section of the wind tunnel at the exit to the exposure chamber using a handheld CPC and found to be homogenously distributed. The dilution assured that upon sampling all dynamic particle processes, such as coagulation or cooling, had decayed and the aerosol was stable. Furthermore the particle concentration could be adjusted by means of the dilution air flow rate.

Measurements were conducted on two consecutive days in August 2006. During the first day, a sodium chloride aerosol was produced and on the second day Diesel soot. During the mornings, all instruments were operating at their basic settings (see Table 1), whereas during afternoon measurements, the instrument were switched to different settings, concerning flow rates and/or DMA used. SMPS-T1 was operated with equal settings throughout all experimental runs, thus providing a reference allowing for a detailed analysis of the influence of instrument settings on measurement results in comparison to SMPS-T1.

Experimental Set Up

During experiments all SMPS's sampled from the exposure chamber via the same sampling line and manifold. The sampling line comprised a 5.85 m long tube, operated at 20 l/min, connected via a T-connector to 1.50 m long tubes, which split the total flow into two 10 l/min flows. The flow rates in the sampling line were intentionally maintained high but within laminar flow conditions to minimize diffusional particle losses within the sampling system. The SMPS's sampled from one end of the short tube via 2 m long electrically conducting flexible tubes, whereas other instruments that measured alongside but are not subject of this paper were connected to the other end (see Figure 1). SMPS-T1 was operated at a constant aerosol flow rate of 0.3 l/min, SMPS-T2 at either 0.3 l/min (basic setting) or 0.6 l/min and SMPS-G1 always at 0.3 l/min, thus resulting in a total sample flow of all instruments of 0.9 l/min or 1.2 l/min, respectively. An additional flow of 9.1 l/min or 8.8 l/min, respectively, was withdrawn from the sampling point to maintain a total flow rate of 10 l/min in the distributing leg of the sampling system. The FMPS operated at a sample flow rate of 10 l/min and was directly connected to the exposure chamber via a 2.5 m long flexible tube. Size dependent particle penetration through the different sections of the sampling lines were calculated for each instrument and used for correction of diffusion losses. The penetration *P* through circular tubes can be expressed as (Gormley and Kennedy, 1949; Soderholm, 1979):

$$P = 0.82 \cdot \exp(-11.5\mu) + 0.10 \cdot \exp(-70\mu) + 0.03 \cdot \exp(-180\mu) + 0.02 \cdot \exp(-340\mu) \quad [1]$$

With the penetration coefficient μ

$$\mu = \frac{D \cdot L_{tube}}{Q} \quad [2]$$

Where Q is the total flow rate through the tube, L_{tube} is the length of the tube and D is the diffusion coefficient (e.g. Hinds, 1999):

$$D = \frac{k \cdot T \cdot C_c}{3\pi \cdot \eta \cdot d_m} \quad [3]$$

Where k is the Boltzman constant ($1.3807*10^{-23}$ J/K), T is the absolute temperature, C_c is the Cunningham slip correction factor (Cunningham, 1910; Kim *et al.*, 2005) η is the viscosity of air and d_m the particle mobility diameter.

The two handheld CPC's operated at 0.7 l/min sample flow and were directly connected to the exposure chamber via short flexible tubes. A correction of the CPC data for diffusion losses was not possible because the instrument delivers only an

integral value, but no size distribution. Only diffusional particle losses in straight tubes were considered, whereas losses in bends and elbows were neglected, although Wang *et al.* (2002) reported that these may be of importance. The evaluation of those losses, however, is not straightforward. Since all instruments, except for the FMPS, were sampling through identical tubing, with identical flow except for the last 2 m flexible tube after the final distribution, the aerosol sampled by all instruments passed through the same bends and elbows. The last 2 m flexible tube, however, introduced the highest diffusional losses, because the total flow rate is here reduced to the sample flow rate of the instruments.

Particle Generation

Particles were generated and injected into the wind tunnel at the opposite end of the exposure chamber. Two different types of aerosols were intentionally produced, sodium chloride (NaCl) and diesel soot.

An atomizer was used to generate the NaCl aerosol. The particle generator included a two component jet that was fed by a 0.4% (by mass) solution of NaCl in DI water. The atomizer produced 1 l/min NaCl aerosol that was injected into the wind tunnel, where it was mixed with approx. 100 l/min dry dilution air from a pressurized air supply. The dilution air dried the aerosol, resulting in 10.8% relative humidity at 21.4°C near the end of the wind tunnel after homogenous mixing. The resulting size distribution of the NaCl aerosol, measured in the exposure chamber with SMPS-T1 is shown in Figure 2 (top). The generated aerosol was very stable throughout the measurements (see small bars of the standard deviations). Total NaCl particle concentrations were on average $1.29*10^5$ cm^{-3} and the size distribution could be fitted with a lognormal distribution using the best fit option of the statistical analysis software SPSS, version 13.0.1. The resulting mode diameter is 34.6 nm, median diameter 51.8 nm and geometric standard deviation approx. 1.71. The correlation coefficient of the fit is $R^2 = 0.995$.

To produce Diesel soot particles, the exhaust pipe of a Diesel engine (aspiration type, 2180 cm^3 Mercedes Benz 220D, 44 kW at 4200 rpm) idling at 1200 rpm was connected to the wind tunnel. The engine exhaust was directly led into the wind tunnel and diluted with approx. 100 l/min filtered room air, resulting in an aerosol temperature between 22.3°C and 23.3°C and relative humidity between 55.4% and 62.9% in the wind tunnel. The generated Diesel aerosol was very stable over time and no significant spatial variation across the cross section of the wind tunnel outlet

was determined with a CPC. The size distribution measured with SMPS-T1 is illustrated in Figure 2 (bottom). The distribution was fitted using SPSS 13.0.1 to a lognormal distribution with a correlation coefficient of R^2 = 0.998, a mode diameter of 82.0 nm, median diameter of 105.9 nm, geometric standard deviation of 1.59 and an average concentration of $1.5*10^6$ cm^{-3}. In another diesel soot measurement, the load of the engine was increased such that larger particles were produced. Furthermore the dilution of the engine exhaust in the wind tunnel was increased to lower the total concentrations. The resulting lognormal size distribution had a mode diameter of 94.7 nm, a median diameter of 119.5 nm, and a geometric standard deviation of 1.56. The distribution was fitted with a correlation coefficient of 0.994. However, it is noteworthy that the geometric standard deviations delivered by all instruments during this and the following diesel soot measurements are in a range from 1.48 to 1.69 (average 1.60). Harris and Maricq (2002) reported a more or less universal σ_g of 1.80 for the non-volatile components of diesel soot. Virtanen *et al*. (2004) measured geometric standard deviations non-volatile diesel soot components in a range between 1.8 and 2.2, depending on engine load. These standard deviations are significantly larger than the ones determined here and give rise to the assumption that the diesel soot particles used in this study were coated with volatile hydrocarbon compounds, causing the geometric standard deviation to drop. This would also have an impact on particle morphology, because the coating makes the particles more compact. SEM images of test particle samples were taken but could not deliver conclusions whether particles were coated with volatile compounds, because those evaporate under vacuum conditions inside the SEM.

Instrumentation and Calibration Check

Mobility particle sizers can cover a size range between approximately 3 nm and 1 µm, depending on their configuration. While the FMPS delivers size distribution data every second, the time resolution of an SMPS is on the order of several minutes. Therefore, the FMPS based technique is more appropriate for relatively fast changing aerosol size distributions while the SMPS based technique gives a much higher size resolution enabling better the fine differentiation of particle modes in a given distribution. The principle of mobility particle sizers is that particles of a defined charge distribution (Fuchs, 1963; Wiedensohler, 1988) get classified inside a mobility analyzer according to their electrical mobility and are subsequently counted. The

known dependence of the charge distribution on particle size is exploited in mobility particle sizers to deconvolute the measured mobility spectrum of an aerosol into the number size distribution (Hoppel, 1978; Fissan *et al.*, 1983). To obtain the mobility distribution, the electric field strength inside the classifier is either sequentially (Fissan *et al.*, 1983) or continuously (Wang & Flagan, 1990) ramped to withdraw a small bandwidth of electrical mobilities. Particles within this bandwidth are counted, commonly with a condensation particle counter.

The two tested Scanning Mobility Particle Sizers were identical, except for the CPC's used. While SMPS-T1 used a water based ultrafine condensation particle counter (TSI, Model 3786; Hering *et al.*, 2005) with a lower detection limit of 2.5 nm, SMPS-T2 was connected to a butanol based CPC (TSI, model 3010) with a lower detection limit of 10 nm. Both instruments were operated with a long column Differential Mobility Analyzer (DMA, TSI, model 3071) as originally introduced by Pui and Liu in 1974. Depending on the flow rate settings, SMPS-T1 and SMPS-T2 delivered size distributions in the size range 13.8 nm ≤ d_p ≤ 749.9 nm (0.3 l/min aerosol, 3 l/min sheath flow) or 9.3 nm ≤ d_p ≤ 437.1 nm (0.6 l/min aerosol, 6 l/min sheath flow; only SMPS-T2). With these SMPS's, size distribution data are available in 64 size channels per decade. Particles were charged with an ^{85}Kr neutralizer (TSI, model 3077). Data were collected and evaluated with the TSI software package *Aerosol Instrument Manager* (version 8.0.0.0).

The Sequential Mobility Particle Sizer (Heim *et al.*, 2004) was equipped with a Vienna-type DMA (Winklmayr *et al.*, 1990) with a replaceable electrode system. By exchanging the electrodes, the covered particle size range can be adjusted. In this study, two differently sized electrode systems were used, a short system (Grimm, M-DMA, 88 mm long) to cover a size range from 5.5 nm to 350.4 nm and a long system (Grimm, L-DMA, 350 mm long) for the size range 11.1 nm – 1083.3 nm. With this SMPS model, size distribution data are available in 44 size channels per decade. The DMA always operates at 0.3 l/min aerosol and 3 l/min sheath flow rate. Particles were charged in a ^{241}Am neutralizer (Grimm, model 5.522) prior to classification. A condensation particle counter (Grimm, model 5.404) with a lower detection limit of 5 nm was connected to the DMA to count the particles downstream. Data were collected with software provided by the manufacturer which also allows for correction of losses in the system. The procedure for data correction is not further specified by the manufacturer.

The FMPS (TSI, model 3091) is based on the Electrical Aerosol Spectrometer (EAS), developed at the University of Tartu, Estonia (Mirme and Tamm, 1991 &1993, Tammet *et al.*, 1998). Particles are charged first in a negative then in a positive unipolar corona charger to obtain a predictable, size dependent charge distribution. The classifier operates similarly to a DMA with the main difference that particles are directly deposited on an array of 22 electrometers along the outer electrode, each one representing a certain electrical mobility bandwidth. With the known charge level of the particles, the measured current of the electrometers is deconvoluted into particle number size distributions (5.6 nm to 562.3 nm, 16 size classes per decade). Unlike in an SMPS, particles of a certain electrical mobility are not counted directly, but the number concentration is inferred from a current measurement, assuming that the charge distribution of the particles is known. The FMPS operates at 10 l/min aerosol and 40 l/min sheath flow rate. Instrument settings are not adjustable; therefore the FMPS was always operated with its default settings. Particle losses inside the FMPS have not yet been subject to detailed analysis and were therefore not corrected. However, diffusional losses inside the instrument are assumed to be small due to the high flow rate and hence low residence time of particles within the instrument.

The Condensation Particle Counters (both TSI, model 3007) used in this study were handheld type CPC's as can e.g. be used for routine measurement of particle concentrations in workplaces. The counters use butanol as working fluid and have a butanol reservoir for approx. 8 hour continuous operation. The counters sample particles between 10 nm and 1 µm at a flow rate of 0.7 l/min (Hämeri *et al.*, 2002). The maximum concentration that can accurately be detected is 10^5 cm^{-3}. The CPC's did not allow for any changes in the settings and therefore always sampled at their default settings. Particle losses in the instrument and the 2 m long sampling tube were not corrected, because no size distributions are recorded by the CPC, which are required to correct for diffusional losses (see equation [1]).

Calibration Check

The calibration of the particle sizers concerning particle size was tested with certified 100 nm PSL particles. SMPS-T1 and SMPS-T2 showed the peak in the 105 nm size bin, SMPS-G1 at 101 nm. Only the FMPS showed it at a too low diameter of 80 nm, which indicated that the sizing accuracy of the FMPS seems to be lower than that of the SMPS's in this study. Since the FMPS does not allow for a size calibration, it was

used with its default settings. A calibration check for the number concentration could not be performed due to the lack of a suitable number concentration standard.

Results

Data fitting of the measured size distributions was necessary because of the different size channel sizes and midpoints determined by the different instruments. Fitting was conducted using the fitting option of the commercial SPSS software, version 13.0.1. A lognormal particle number size distribution which is fully characterized by three parameters: total number concentration C_N, count median diameter d_{CMD}, and geometric standard deviation σ_g (e.g. Hinds, 1999), was used for the fit:

$$\frac{dN}{d\log(d_p)} = \frac{1}{\sqrt{2\pi}\cdot d_p \cdot \log(\sigma_g)} \cdot \exp\left[\frac{\log^2\left(\frac{d_p}{d_{CMD}}\right)}{2\cdot\log^2(\sigma_g)}\right] \cdot C_N \qquad [4]$$

The three significant parameters C_N, d_{CMD}, and σ_g of the fitted lognormal size distribution curves from the different instruments were compared. Furthermore the mode diameters, i.e. the diameter where the peak appeared in the distribution, were compared with each other. It is noteworthy that count median diameter and mode diameter are only equal in a normal distribution, but different in a lognormal distribution. Correlation coefficients between the fit and the measured curves were between 0.990 and 1.0 for the SMPS's and between 0.963 and 0.995 for the FMPS, showing that the assumption of lognormal distribution was justified. Deviations of the fit from the measured data were mainly observed towards the boundaries of the distributions, where concentrations were low and measurements therefore prone to higher uncertainty.

Sodium Chloride

Sodium chloride (NaCl) particles were generated and sampled for two continuous hours during two experimental runs. During the first run, all instruments were set to their basic settings, while during the second run, instrument settings were varied as listed in Table 1. The measured data were averaged for each instrument and mathematically fitted under the assumption of a lognormal distribution according to equation [4], using SPSS software, version 13.0.1. The parameters of the resulting lognormal distributions are listed in Table 2 along with the results from the CPC's. Total concentrations of the size distributions are integrals within the size limits of

SMPS-T1, i.e. from 13.8 nm to 749.9 nm. Correlation coefficients R^2 between 0.990 and 0.999 for all SMPS's indicate that the assumption of a lognormal distribution was justified. As the graph in Figure 2 (top) shows, for NaCl measurements, the fit slightly deviated only for particles below approximately 20 nm. The correlation coefficient for the FMPS was lower than those of all SMPS's. The FMPS size distributions consistently exhibited a small peak at around 10 nm and a little dent at approximately 25 nm which don't seem to be real but rather caused by hardware or software failure. These deviations seem to have caused the correlation coefficient to drop.

Basic Instrument Settings

The fitted size distributions of the different instruments with basic instrument settings are shown in Figure 3 for the first set of NaCl measurements. The fitted curves were used to obtain the total number concentrations by integrating the number size distributions within the size limits of SMPS-T1 (13.8 nm ≤ d_p ≤ 749.9 nm). As listed in Table 2, the concentrations of SMPS-T1, SMPS-T2 and the FMPS agreed very well, whereas SMPS-G1 delivered approximately 42% higher concentration. The concentrations measured simultaneously with two handheld CPC's were 25% and 37%, respectively, lower than the concentration measured with SMPS-T1. It should be noted though that the CPC's were operated at approximately their concentration limits of 10^5 cm^{-3}. The graph in Figure 3 shows that the size distributions, measured by SMPS-T1, SMPS-T2 and FMPS are very similar with only the mode diameter of the FMPS shifted to smaller particles. The size distribution of SMPS-G1 is elevated towards higher concentrations with the mode diameter slightly shifted towards a smaller diameter. The similarity of SMPS-T1, SMPS-T2 and FMPS is not very surprising since all three instruments are from the same manufacturer. SMPS-T1 and SMPS-T2 show a slight deviation, despite the fact that both instruments were identical and operated with equal settings. While SMPS-T1 showed a size distribution with a mode diameter of 34.6 nm and a geometric standard deviation of 1.71, SMPS-T2 delivered a broader distribution with σ_g = 1.85 with approximately 10% lower peak concentration and shifted to a mode diameter of 32.2 nm. SMPS-G1 delivered a broader distribution (σ_g = 1.860) than SMPS-T1 with an approximately 15% higher peak concentration. The mode of SMPS-G1 was shifted to 29.4 nm compared with SMPS-T1 at 34.6 nm. The FMPS delivered a significantly broader distribution with σ_g = 2.047 than SMPS-T1. The peak concentration of the FMPS was rather comparable with SMPS-T2, but the mode diameter further shifted to 27 nm. The

FMPS mode diameter is thus approximately 22% smaller than the mode diameter measured with SMPS-T1. This deviation is comparable with the deviation observed during calibration check with 100 nm PSL particles, where the FMPS delivered a peak at 80 nm and gives rise to the assumption that the sizing of the FMPS is less accurate than the sizing of all tested SMPS's.

Different Instrument Settings

For these measurements, SMPS-T2 was operated with higher aerosol and sheath flow rate of 0.6 l/min and 6 l/min, respectively. The DMA of SMPS-G1 was switched from the long L-DMA to the short M-DMA after one hour of the two hour measurement. The fitted size distributions from the different instruments are illustrated in Figure 4 and the parameters of the fitted size distributions listed in Table 2. The total number concentration of SMPS-T1 was lowest among all particle sizers. The increase in the flow rate of SMPS-T2 seemed to also increase the total measured concentration, despite diffusion correction in both SMPS-T1 and SMPS-T2. The total concentration of SMPS-T2 was approximately 34% above that of SMPS-T1. Total concentrations measured with L-DMA and M-DMA in SMPS-G1 were very similar, but 71% and 79%, respectively, higher than the SMPS-T1 concentrations. This is in agreement with findings by Helsper et al. (2008), who found that the Grimm SMPS along with M-DMA showed on average 48% higher concentrations than a condensation particle counter, which however agreed very well with the number concentration of the TSI SMPS with long DMA. It can only be speculated what caused the large deviation between the SMPS-G1 and SMPS-T1. As the deviation between SMPS-T1 and SMPS-T2 with different flow rate settings shows, the SMPS's are very sensitive to changes in flow rate. A likely reason for the discrepancy is therefore inaccurate flow rate calibration of one or more SMPS during the measurement. Helsper et al. (2008) assumed that the different algorithms used for data inversion, the different charge distribution used by TSI and Grimm or the different polarity of particles sampled by TSI (negative) and Grimm (positive) SMPS's may cause the discrepancy. The total concentration of the FMPS was approximately 15% above the SMPS-T1 concentration. Concentrations measured with the two handheld CPC's were closest to the SMPS-T1 values and approximately 15% and 8%, respectively, below them. The size distributions in Figure 4 clearly show that SMPS-T1 measured the narrowest distribution with a standard deviation of 1.63, the largest mode diameter of 37.2 nm and the lowest total concentration of $1.19*10^5$ cm^{-3}.

The size distribution of SMPS-T2, which was operated with higher flow rates than during the first experimental run, delivered a smaller peak diameter of 28.9 nm, a broader distribution with σ_g = 1.85 and an approximately 10% higher maximum concentration.

The change of the DMA in SMPS-G1 only caused a small, insignificant change in the measured size distribution. Like in the first experimental runs, SMPS-G1 delivered significantly smaller peak diameters (38% and 26%, respectively) than SMPS-T1. The distributions delivered by SMPS-G1 were noticeably broader than with SMPS-T1. The mode diameters of SMPS-G1 with short and long DMA, however, agreed well with that of SMPS-T2.

The FMPS delivered a slightly smaller mode diameter of 34.0 nm than SMPS-T1 (37.2 nm) with almost identical peak height, but a broader distribution with σ_g = 1.85. The detection of a smaller mode is consistent with the previous NaCl measurement and the calibration check, although the deviation to SMPS-T1 is smaller (approximately 9%) here.

Diesel Soot

Three experimental runs were conducted with Diesel soot particles. The measured data were fitted with lognormal size distributions (equation [4]) using SPSS software, version 13.0.1. As Figure 2 (bottom) shows, the data followed the lognormal distribution almost perfectly. During the first two runs, the Diesel engine settings (idling at 1200 rpm) and dilution air flow rate in the wind tunnel were identical, whereas the engine load and dilution air flow rate were both increased during the third run, resulting in a larger mode diameter and lower concentration of the resulting particle size distribution. During the first run, all instruments were sampling with their basic settings (equal to first run with NaCl). Only the DMA of SMPS-G1 was changed from L-DMA to M-DMA during the measurement. During the second run, aerosol and sample flow rate of SMPS-T2 were increased to 0.6 l/min and 6 l/min, respectively. During the third run, all mobility particle sizers were set back to their original settings (equal to first run with NaCl). The SMPS-T1 settings remained unchanged throughout all measurements. Measurements with handheld CPC's did not deliver meaningful results, because the particle number concentration exceeded their maximum concentrations by more than an order of magnitude during the first two runs and by a factor of three to six during the third run. During each experimental run, data were

taken for two consecutive hours and the parameters of the fitted lognormal distributions are listed in Table 3. Total concentrations of the size distributions are integrals within the size limits of SMPS-T1, i.e. from 13.8 nm to 749.9 nm. The correlation coefficients of the fits were higher than in the case of NaCl, between 0.994 and 1.0 for SMPS's and between 0.990 and 0.995 for the FMPS, i.e. justifying the assumption of lognormal distributions.

Basic Instrument Settings – Engine Idling

The fitted size distributions, obtained with the different mobility particle sizers are shown in Figure 5 and their parameters summarized in Table 3. The total number concentration, obtained from integration over the fitted curves, was lowest for SMPS-T2, approximately 19% below SMPS-T1. The difference in the number concentration with the long and short DMA in SMPS-G1 was approximately 11% and these concentrations 20% and 35%, respectively, above SMPS-T1. The FMPS delivered an approximately 32% higher total concentration. The graph in Figure 5 illustrates that SMPS-T1, SMPS-T2 and SMPS-G1 along with the long DMA show very similar sizing concerning the mode diameter, i.e. 82.0 nm with SMPS-T1, 85.1 nm with SMPS-T2 and 82.8 nm with SMPS-G1. However SMPS-G1 along with the short DMA exhibited a smaller mode diameter at 75.4 nm. As in the previous measurements and the calibration check, the FMPS delivered the smallest mode diameter of 69.8 nm. Compared with SMPS-T1 this is approximately 15% smaller. The deviations between the mean diameters are in a similar range as found by Dahmann *et al.* (2001). The FMPS delivered the highest peak concentration, followed by SMPS-G1 (long DMA), SMPS-G1 (short DMA), SMPS-T1 and SMPS-T2. As in the previous measurements, SMPS-G1 delivered the broadest distributions with σ_g = 1.69 along with the long DMA and σ_g = 1.67 with the short DMA. The smallest standard deviation was measured by the FMPS with σ_g = 1.56. Due to the broad measured distribution, SMPS-G1 with the long DMA delivered the highest total concentration ($2.03*10^6$ cm^{-3}), closely followed by the FMPS ($1.98*10^6$ cm^{-3}). The lowest total concentration was measured by SMPS-T2 ($1.22*10^6$ cm^{-3}). SMPS-T1 and SMPS-T2 delivered comparable size distributions concerning mode and median diameter as well as standard deviation. However, peak height and total concentration differed by approximately 19%, despite the exactly same settings of both samplers. SMPS-G1 delivered similar size distributions with the two different DMA's. The long DMA measured a slightly larger peak diameter (~10%) and a slightly wider distribution

(σ_g = 1.69 compared with 1.67) than the short DMA. Only the broader distribution of the long DMA compared with the short DMA is consistent with the previous NaCl measurement, whereas the changes in diameter and concentration are reverse. The differences, however, are so small that they cannot clearly be linked to a different response of the DMA's to different particle morphologies. It is interesting to note that the FMPS now delivered the lowest geometric standard deviation, whereas for NaCl it was always significantly higher than all others. This may have different reasons, one being the different reaction of SMPS's and FMPS to the different morphologies of NaCl and diesel soot particles. Another reason may also be a changing response of the FMPS for different particle sizes.

Different Instrument Settings – Engine Idling

During the second set of measurements with Diesel soot, SMPS-T2 was switched to higher flow rates (0.6 l/min aerosol and 6 l/min sheath flow). SMPS-G1 was operated with the long DMA throughout the measurements. The measured size distributions are shown in Figure 6. The lowest total concentration was measured with SMPS-T1. As in the previous cases, the concentration of SMPS-T2 was noticeably (24%) higher, which was obviously caused by the higher flow rate. The total concentrations of SMPS-G1 (long DMA) and the FMPS were identical and 36% higher than the concentration of SMPS-T1. SMPS-T1 delivered almost exactly the same parameters as during the first run with equal engine settings. The illustration in Figure 6 shows that the sizing of SMPS-T1, SMPS-T2 and SMPS-G1 was very similar with a scatter of only ±2%. SMPS-G1 delivered the broadest distribution and highest peak (approximately 20% higher than SMPS-T1). This is consistent with all previous measurements. The delivered size distribution of SMPS-G1 was very consistent with the one measured in the first run. In contrast to the earlier measurement with lower flow rates, where SMPS-T2 showed a lower concentration and slightly larger mode diameter than SMPS-T1, now SMPS-T2 showed a higher concentration and slightly smaller mode diameter. This finding is consistent with the results from the earlier NaCl measurements, where the increase of the SMPS-T2 flow rates also caused the measured concentration value to increase, while the mode diameter decreased. Like in the earlier Diesel soot measurement, the FMPS exhibited the highest peak, the smallest mode diameter and the narrowest distribution, i.e. the lowest geometric standard deviation. The delivered parameters from the FMPS during the two experimental runs with equal engine settings were very consistent.

Basic Instrument Settings – Engine with Load

An artificial load was added to the engine and the dilution ratio in the wind tunnel increased, resulting in an increased mode diameter and a lower concentration of the size distribution (Figure 7 and Table 3). Again the total concentration of SMPS-T1 was lowest but only 11% lower than the one of SMPS-T2. SMPS-G1 with long DMA and FMPS delivered very similar concentrations, but both significantly higher (74% and 71%, respectively) than the SMPS-T1 concentration. The sizing of the three SMPS's was almost identical with the smallest diameter of 91.4 nm measured by SMPS-T2, followed by SMPS-G1 (91.5 nm) and SMPS-T1 with 94.7 nm. SMPS-G1 measured the broadest distribution with σ_g = 1.61, while SMPS-T1 (σ_g = 1.56) and SMPS-T2 (σ_g = 1.57) delivered slightly narrower distributions. Despite equal settings of the two largely identical SMPS-T1 and SMPS-T2 they delivered slightly deviating size distributions. However, these deviations are insignificant (<10% in total concentration, <3% in mode diameter).

Like in the earlier Diesel soot measurements, the FMPS delivered the smallest standard deviation (σ_g = 1.48) with a noticeably smaller mode diameter (80.6 nm) and very high concentration. This is contrary to the NaCl measurements, where the FMPS delivered only slightly smaller mode diameters but significantly broader distributions with total concentrations comparable with SMPS-T1. This consistent shift of the FMPS size distribution towards smaller particle sizes, narrower distributions, and higher concentrations give rise to the assumption that FMPS and SMPS show different reactions to diesel soot and NaCl particles. As mentioned earlier this may be due to different morphology or different size.

Summary and Conclusions

Four different mobility particle sizers (two TSI-SMPS's, one Grimm SMPS and one TSI-FMPS) were challenged with NaCl and Diesel soot particles. While SMPS's generally serve to measure rather stable particle size distributions, the high time resolution of the FMPS allows for measuring quickly changing distributions. However, the FMPS size resolution of 16 size channels per decade is lower than that of the SMPS's, namely 44 channels per decade in case of the Grimm device and 64 channels per decade in case of the TSI SMPS. One TSI SMPS (SMPS-T1) was always operated with identical settings and therefore served as an internal reference. Settings of the two other SMPS's were varied during the experiments. FMPS settings

were fixed and could not be varied. Generally, a good agreement was found concerning the sizing of the scanning and sequential particle sizers in the test. Only the FMPS consistently delivered smaller particle sizes with the mode diameters between 9% and 22% below those determined with SMPS-T1. All instruments showed repeatable results. However, the measured concentration levels varied significantly from instrument to instrument. Due to a lack of a standard for the number concentration, the “correct” concentration level could not be determined. It was observed that accurate flow rate setting is crucial for precise concentration determination as some of the measured deviations of SMPS number concentrations are assumed to be caused by inaccurate flow rates. This is consistent with earlier findings by Dahmann *et al.* (2001). Systematic differences in the sizing of the SMPS’s depending on the particle morphology could not be observed, however there is clear evidence that SMPS’s and FMPS react differently to the tested NaCl and Diesel soot particles. Reasons for the different reactions found here can be the different morphology of NaCl and diesel soot or the different particle sizes.

This comparison showed that comparable measurement results within about 30% accuracy can be achieved but it has to be taken into account that this exercise was conducted by experienced researchers and workplace hygienists under controlled conditions. Therefore firstly improvements in standardisation and harmonisation are needed and secondly comparison facilities have to be implemented.

A detailed analysis of the findings is given below for the different instruments in the test.

Handheld CPC – TSI model 3007

Two identical handheld CPC’s were used in this test series to compare the total measured concentrations with those delivered by the mobility particle sizers. The CPC’s could only be used during NaCl measurements, because the diesel soot concentrations exceeded the concentration limit of the devices. The two CPC’s agreed very well with each other with less than ±5% deviation. This is a much better agreement than found by Matson *et al.* (2004) who compared the model 3007 CPC with a very similar handheld P-Trak CPC and found agreement only within ±20%. The agreement between the CPC readings and the total concentrations from the mobility particle sizers was not as good. Compared with SMPS-T1, the two CPC’s showed 8.8% and 20.2%, respectively, lower concentrations. The different particle

size ranges of the CPC's (10 nm to 1 µm) and the other tested instruments did not have a significant impact on the total measured concentrations because of very low number concentrations in the non-overlapping size range. It should be noted that the CPC's were operated near the specified concentration limit of 10^5 cm^{-3} and Hämeri *et al.* (2002) have reported that the CPC 3007 starts to under-estimate particle concentrations when operated near its concentration limit. Concerning the differences between the concentrations measured with mobility particle sizers, the agreement with the CPC's can still be considered as acceptable. Handheld CPC's can therefore be used to deliver quick and easy estimates of particle number concentrations at various locations.

SMPS – TSI model 3080

Two largely identical TSI SMPS's (SMPS-T1 and SMPS-T2) were investigated. The only difference was that both operated with different condensation particle counters. SMPS-T1, equipped with a water-based UCPC (TSI model 3786) was continuously operated with equal settings, while the flow rates of SMPS-T2, equipped with a butanol based CPC (TSI model 3010) was switched between low flow (0.3 l/min aerosol and 3 l/min sheath flow) and high flow (0.6 l/min and 6 l/min). With equal settings, the two instruments produced very comparable results. However SMPS-T2 consistently delivered slightly larger geometric standard deviations, which might be attributed to the DMA manufacturing accuracy that affects the DMA transfer function. On average, the standard deviation of SMPS-T2 was 2.8% larger than the one of SMPS-T1. The deviation was more pronounced during the NaCl measurements where the difference was about 8%, whereas during Diesel soot measurements it was only about 1%. The SMPS has shown to be very sensitive to accurate flow rate settings. Only when the flow rates were very carefully checked and adjusted, the measured concentrations were almost identical, whereas deviations within approximately ±20% in the total concentrations were observed without prior flow rate adjustment.

When SMPS-T2 was switched to the higher flow rates, a consistent and noticeable shift in the measured size distribution could be observed even though the software was set to correct the data for flow rate dependent diffusion losses. The mode diameter of the distribution was shifted towards smaller particles. The size shift,

however, was rather small. More pronounced was the change in the total concentration which was on average 29.0% higher when SMPS-T2 was operated with a higher flow rate.

The agreement between the two instruments can be considered as good concerning sizing of the particles. The observed deviations, although some of them appear to be systematic, are small and certainly fall within the measurement uncertainty. The differences in the measured concentrations can be more critical. When operating two instruments at identical settings, careful flow calibration is highly recommended.

SMPS – Grimm SMPS+C

A Grimm SMPS+C was investigated with two different DMA's: a long L-DMA and a shorter M-DMA. The results from the two DMA's agreed well with each other. Only small differences were observed. The long DMA seemed to deliver slightly larger (5%) geometric standard deviations. Deviations in the sizing and concentrations do not seem to be systematic and certainly fall within the measurement uncertainty. A dependence of the results on particle material was not observed.

Comparison of Grimm SMPS-G1 with the TSI SMPS-T1 showed that the sizing of the two instruments was comparable within less then 10% deviation, although the Grimm SMPS seemed to tend to smaller particle sizes. However, concentrations and geometric standard deviations of SMPS-G1 were consistently higher than those of SMPS-T1. With the long DMA, the geometric standard deviation was on average 10.8% larger and the total concentration 51.6%. The deviation of both showed a very large scatter from +2.9% to +29.6% for the standard deviation and from +35.3% to +74.4% for the concentration. With the short DMA the standard deviation was on average 12.8% higher and the total concentration 49.8%. This is in very good agreement with the findings of Helsper et al. (2008) who found that their Grimm SMPS with short DMA delivered 48% higher number concentrations than a simultaneously sampling CPC, while a TSI SMPS with long DMA was in good agreement with the CPC reading. The average standard deviation includes differences from +4.9% to +20.8%, while the concentrations differed from -20.7% to +79.0%.

FMPS – TSI model 3091

The FMPS consistently delivered the smallest mode diameters of all instruments and seems to underestimate particle diameter at least in the sub-100 nm size range. This

was also verified in a calibration check, where 100 nm PSL particles exhibited a peak at 80 nm. On average the FMPS underestimated the mode diameter by approximately 15% and the CMD by approximately 17% compared with SMPS-T1. The measured size distributions provide evidence that the FMPS response was different for the two different particle sources in the test – NaCl and diesel soot. While during NaCl measurements, the FMPS always provided the narrowest distributions, i.e. the lowest geometric standard deviation, it consistently provided the widest distributions when challenged with Diesel soot. Furthermore, the measured concentration levels were comparable with the SMPS-T1 levels with NaCl, but significantly larger with Diesel soot. This qualitatively compares well with Johnson *et al.* (2003) who compared the response of an Engine Exhaust Particle Sizer (EEPS, TSI model 3090), which uses exactly the same hardware as the FMPS, with the number concentration from a CPC (TSI, Model 3022) and the size distribution measured with an SMPS. For the number concentration measurements, the instruments were connected to a spark aerosol generator and the integrated EEPS size distributions delivered approximately 50% higher total concentrations than the CPC measurements. In their study, number size distributions of a Diesel engine exhaust were measured with EEPS and SMPS (model not specified). They found a fairly good comparison of the size distributions within the size range of interest for most Diesel exhaust measurements, but a noticeable deviation was observed for particle sizes above approximately 80 nm, where the EEPS underestimated particle concentrations. This agrees well with the findings in this study, where for Diesel soot, the particle concentrations measured with the FMPS were below the SMPS concentrations for particle sizes above approx. 100 nm (Figures 5 to 7). It can only be speculated about the reason for the observed discrepancy. One possible reason may be the different morphologies of NaCl and Diesel soot particles, causing differences in particle charging. While the SMPS's make use of bipolar charging by either ^{85}Kr (TSI) or ^{241}Am (Grimm), the FMPS uses two consecutive unipolar corona chargers of opposite polarity to obtain a predictable charge distribution. It has been reported by several researchers that charging is affected by particle morphology. While Wiedensohler (1988) assumed spherical particles in his widely accepted estimation of bipolar particle charging efficiency, Wen *et al.* (1984) used a charging equivalent diameter for agglomerates as a function of number and size of the primary particles. This equivalent diameter can be noticeably different from the mobility diameter. Oh *et*

al. (2004) studied the effect of fractal dimension on unipolar diffusion charging of TiO_2 agglomerates. They found the charge quantity of particles to decrease, as the sintering temperature increased during particle generation. These findings indicate that particle shape can have a significantly different impact on unipolar and bipolar particle charging which would need to be taken into account for data deconvolution. A correction of measured data for agglomerate charging is currently only possible for SMPS-T1 and SMPS-T2 with a recently released software upgrade (Aerosol Instrument Manager, version 8.0.0.0), which is based on a theory published by Lall and Friedlander (2006a & 2006b) and only valid under very specific assumptions. Since this correction is only available for the one type SMPS but not for the other and not for the FMPS and since it is further unknown whether the diesel soot morphology meets the assumptions in the model, data were taken as they were and not subject to further agglomerate charging correction.

Another likely reason for the discrepancy is the different particle sizes from the two sources, as Johnson et al. (2003) reported a size dependence of the discrepancy between EEPS and SMPS. While NaCl particles show a peak at about 35 nm, the diesel soot peak was at 82 nm, when the engine was idling and at 95 nm with engine under load.

Acknowledgement

This work was supported by the German Federal Ministry of Education and Research (BMBF) as part of the *NanoCare* project.

Bibliography

R.W. Atkinson, H.R. Anderson, J. Sunyer, J. Ayres, M. Baccini, J.M. Vonk, A. Boumghar, F. Forastiere, B. Forsberg, G. Touloumi, J. Schwartz, K. Katsouyanni (2001). Accute effects of particulate air pollution on respiratory admissions – Results from the APHEA 2 project. *Am. J. Resp. Crit. Care* **164**: 1860-1866

E. Cunningham (1910). On the velocity of steady fall of spherical particles through fluid medium. *Proc. R. Soc. London* Ser. A **83**: 357-365

D. Dahmann, G. Riediger, J. Schletter, A. Wiedensohler, S. Carli, A. Graff, M. Grosser, M. Hojgr, H.G. Horn, L. Jing, U. Matter, C. Monz, T. Mosimann, H. Stein,

B. Wehner, and U. Wieser (2001). Intercomparison of mobility particle sizers (MPS). *Gefahrstoffe – Reinhaltung der Luft* **61**: 423-427

D.W. Dockery, C.A. Pope, X. Xu, J.D. Spengler, J.H. Ware, M.E. Fay, B.G. Ferris, F.E. Speizer (1993). An association between air pollution and mortality in six U.S. cities. *New Engl. J. Med.* **329**: 1753-1759

K. Donaldson, X.Y. Li, W. Macnee (1998): Ultrafine (nanometer) particle mediated lung injury. *J. Aerosol Sci.* **29**:553-560

H. Fissan, C. Helsper and H.J Thielen (1983). Determination of particle size distributions by means of an electrostatic classifier. *J. Aerosol Sci.* **14**:354-357

N.A. Fuchs (1963): On the stationary charge distribution on aerosol particles in bipolar ionic atmosphere. *Geofis. Pura appl.* **56**: 185-193

P.G. Gormley and M. Kennedy (1949). Diffusion from a stream flowing through a cylindrical tube. *Proc. R. Irish Acad.* **52A**: 163-169

S.J. Harris, M.M. Maricq (2001): Signature size distributions for diesel and gasoline engine exhaust particulate matter. *J. Aerosol Sci.* **32**: 749-764

K. Hämeri, I.K. Koponen, P.P. Aalto, M. Kulmala (2002). Technical Note: The particle detection efficincy of the TSI-3007 condensation particle counter. *J. Aerosol Sci.* **33**: 1463-1469

M. Heim, G. Kasper, G.P. Reischl, C. Gerhart (2004). Performance of a new commercial electrical mobility spectrometer. *Aerosol Sci. Technol.* **38:** 3-14

C. Helsper, H.G. Horn, F. Schneider, B. Wehner, A. Wiedensohler (2008): Intercomparison of five mobility particle size spectrometers for measuring atmospheric submicrometer aerosol particles. *Gefahrstoffe – Reinhaltung der Luft* **68**: 475-481

S.V. Hering, M.R. Stolzenburg, F.R. Quant, D.R. Oberreit, P.B. Keady (2005). A laminar-flow, water-based condensation particle counter (WCPC). *Aerosol Sci. Technol.* **39**:659-672

W.C. Hinds (1999). *Aerosol Technology: Properties, Behavior, And Measurement of Airborne Particles*. John Wiley & Sons, New York.

W.A. Hoppel (1978). Determination of the aerosol size distribution from the mobility distribution of the charged fractions of aerosols. *J. Aerosol Sci.* **9**: 41-54

T. Johnson, R. Caldow, A. Pöcher, A. Mirme, D. Kittelson (2003): An engine exhaust particle sizer™ spectrometer for transient emission particle measurements. *9th Diesel Engine Emissions Reduction (DEER) Workshop 2003, Newport, RI, USA*

J.H. Kim, G.W. Mulholland, S.R. Kukuck, D.Y.H. Pui (2005). Slip correction measurements of certified PSL nanoparticles using a nanometer differential mobility analyzer (Nano-DMA) for Knudsen number from 0.5 to 83. *J. Res. Natl. Inst. Stand. Technol.* **110**: 31

P.D. Kinney, D.Y.H. Pui, G.W. Mulholland, N.P. Bryner (1991). Use of the electrostatic classification method to size 0.1 µm SRM particles – a feasibility study. *J. Res. Natl. Inst. Stand. Technol.* **96**:147-176

E.O. Knutson and K.T. Whitby (1975). Aerosol classification by electrical mobility analysis: Apparatus, Theory, and Applications. *J. Aerosol Sci.* **6**: 443-451

W. Koch, G. Pohlmann, K. Schwarz (2008): A reference number concentration generator for ultrafine aerosols based on Brownian coagulation. *J. Aerosol Sci.* **39**: 150-155

W.G. Kreyling, M. Semmler, F. Erbe, P. Mayer, S. Takenaka, H. Schulz, G. Oberdörster, A. Ziesenis (2002). Translocation of ultrafine insoluble iridium particles from lung epithelium to extrapulmonary organs is size dependent but very low. *J. Toxicol. Env. Health* **65:**1513-1530

T.A.J. Kuhlbusch, S. Neumann, H. Fissan (2004): Number size distribution, mass concentration, and particle composition of PM1, PM2.5 and PM10 in bagging areas of carbon black production. *J. Occup. Env. Hyg.* **1**: 660-671

T.A.J. Kuhlbusch, H. Fissan (2006): Particle characteristics in the reactor and pelletizing areas of carbon black production. *J. Occup. Env. Hyg.* **3**: 558-567

T.A.J. Kuhlbusch, H. Fissan, C. Asbach (2009): Nanotechnologies and environmental risks. Eds.: I. Linkov, J. Steevens, *In: Nanomaterials: Risks and Benefits*, Springer Science + Business Media B.V., p. 233-243

A.A. Lall, and S.K. Friedlander (2006a). On-line measurement of ultrafine aggregate surface area and volume distributions by electrical mobility analysis: I. Theoretical analysis. *J. Aerosol Sci.* **37**: 260

A.A. Lall, M. Seipenbusch, and S.K. Friedlander (2006b). On-line measurement of ultrafine aggregate surface area and volume distributions by electrical mobility analysis: II. Comparison of measurements and theory. *J. Aerosol Sci.* **37**: 272

U. Matson, L.E. Ekberg, A. Afshari (2004). Measurement of Ultrafine Particles: A comparison of two handheld condensation particle counters. *Aerosol Sci. Technol.* **38:** 487-495

A. Mirme and E. Tamm (1991). Comparison of sequential and parallel measurement principles in aerosol spectrometry. *J. Aerosol Sci.* **22S1**: S331-S334

A. Mirme and E. Tamm (1993). Electric Aerosol Spectrometer. Calibration and error account. *J. Aerosol Sci.* **24S1**: S211-S212

G.W. Mulholland, M.K. Donnelly, C.R. Hagwood, S.R. Kukuck, V.A. Hackley, D.Y.H. Pui (2006). Measurement of 100 nm and 60 nm particle standards by differential mobility analysis. *J. Res. Natl. Inst. Stand. Technol.* **111**:257-312

G. Oberdörster (2000). Toxicology of ultrafine particles: in vivo studies. *Philos. T. R. Soc. A*, **358**: 2719-2740

G. Oberdörster, Z. Sharp, V. Atudorei, A. Elder, R. Gelein, W. Kreyling, C. Cox (2004). Translocation of inhaled ultrafine particles to the brain. *Inhal. Toxicol.* **16**: 437-445

H. Oh, H. Park, and S. Kim (2004). Effect of particle shape on the unipolar diffusion charging of nonspherical particles. *Aerosol Sci. Technol.* **38**: 1045-1053

K. Park, F. Cao, D.B. Kittelson, P.H. McMurry (2003): Relationship between particle mass and mobility for diesel exhaust particles, *Environ. Sci. Technol.* **37**: 577-583

A. Peters, H.E. Wichmann, T. Tuch, J. Heinrich, J. Heyder (1997). Respiratory effects are associated with the number of ultrafine particles. *Am. J. Resp. Crit. Care* **155**: 1376-1383

Y.H. Pui and B.Y.H. Liu (1974). A submicron aerosol standard and the primary absolute calibration of the condensation nuclei counter. *J. Colloid Interface Sci.* **47**: 155-171

A. Reineking and J. Porstendörfer (1986). Measurement of particle loss functions in a differential mobility analyzer (TSI, Model 3071) for different flow rates. *Aerosol Sci. Technol.* **27:**483-486

S.C. Soderholm (1979): Analysis of Diffusion Battery Data. *J. Aerosol Sci.* **10**: 163-175

H. Tammet, A. Mirme, and E. Tamm (1998). Electrical Aerosol Spectrometer of Tartu University *J. Aerosol Sci.* **29S1**: S427-S428

A.K.K. Virtanen, J.M. Ristimki, K.M. Vaaraslahti, J. Keskinen (2004): Effect of engine load on diesel soot particles. *Environ. Sci. Technol.* **38**:2551-2556

J. Wang, R.C. Flagan, J.H. Seinfeld (2002): Diffusional losses in particle sampling systems containing bends and elbows. *J. Aerosol Sci.* **33**: 843-857

S.C. Wang, R.C. Flagan (1990). Scanning electrical mobility spectrometer. *Aerosol Sci. Technol.* **13**:230-240 (1990)

H.Y. Wen, G.P Reischl, G. Kasper (1984). Bipolar diffusion charging of fibrous aerosol particles –II. Charge and electrical mobility measurements on linear chain aggregates. *J. Aerosol Sci.* **15**: 103-122

A. Wiedensohler (1988). An approximation of the bipolar charge distribution for particles in the submicron size range. *J. Aerosol Sci*. **19**: 387-389

W. Winklmayr, G. P. Reischl, A. O. Lindner and A. Berner (1991). A new electromobility spectrometer for the measurement of aerosol size distributions in the size range from 1 to 1000 nm. *J. Aerosol Sci.* **22**: 289 - 296

Figure Index

SMPS-G1 with L-DMA; curves represent fits over average of two hour measurements

Figure 7: Fitted size distributions for Diesel soot aerosol from engine under load; higher dilution of exhaust than in previous cases, measured with the four different mobility particle sizers in the test with similar settings; size distributions shown in the size limits of the respective instrument; curves represent fits over average of two hour measurements

Table Index

Figure 1

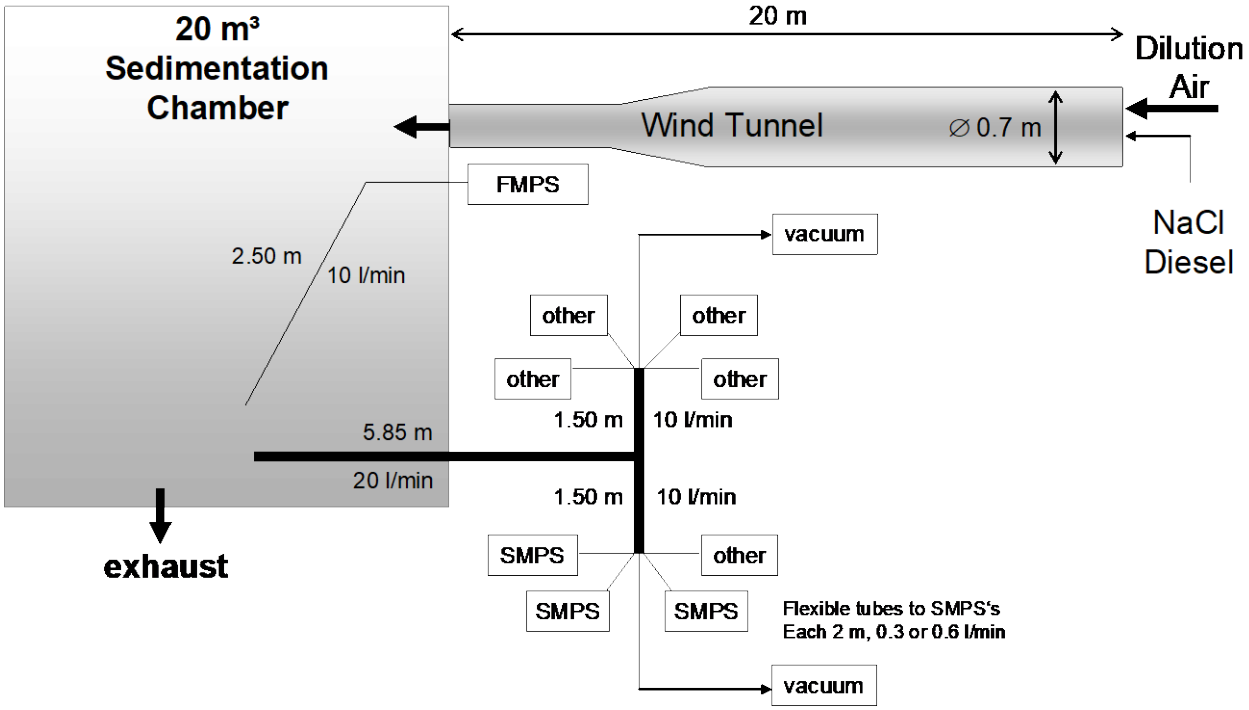
20 m³
Sedimentation
Chamber
20 m
Dilution
Air
Wind Tunnel
∅ 0.7 m
FMPS
NaCl
Diesel
2.50 m
10 l/min
vacuum
other
other
other
other
1.50 m
10 l/min
5.85 m
20 l/min
1.50 m
10 l/min
exhaust
SMPS
other
SMPS
SMPS
Flexible tubes to SMPS's
Each 2 m, 0.3 or 0.6 l/min
vacuum

Figure 2

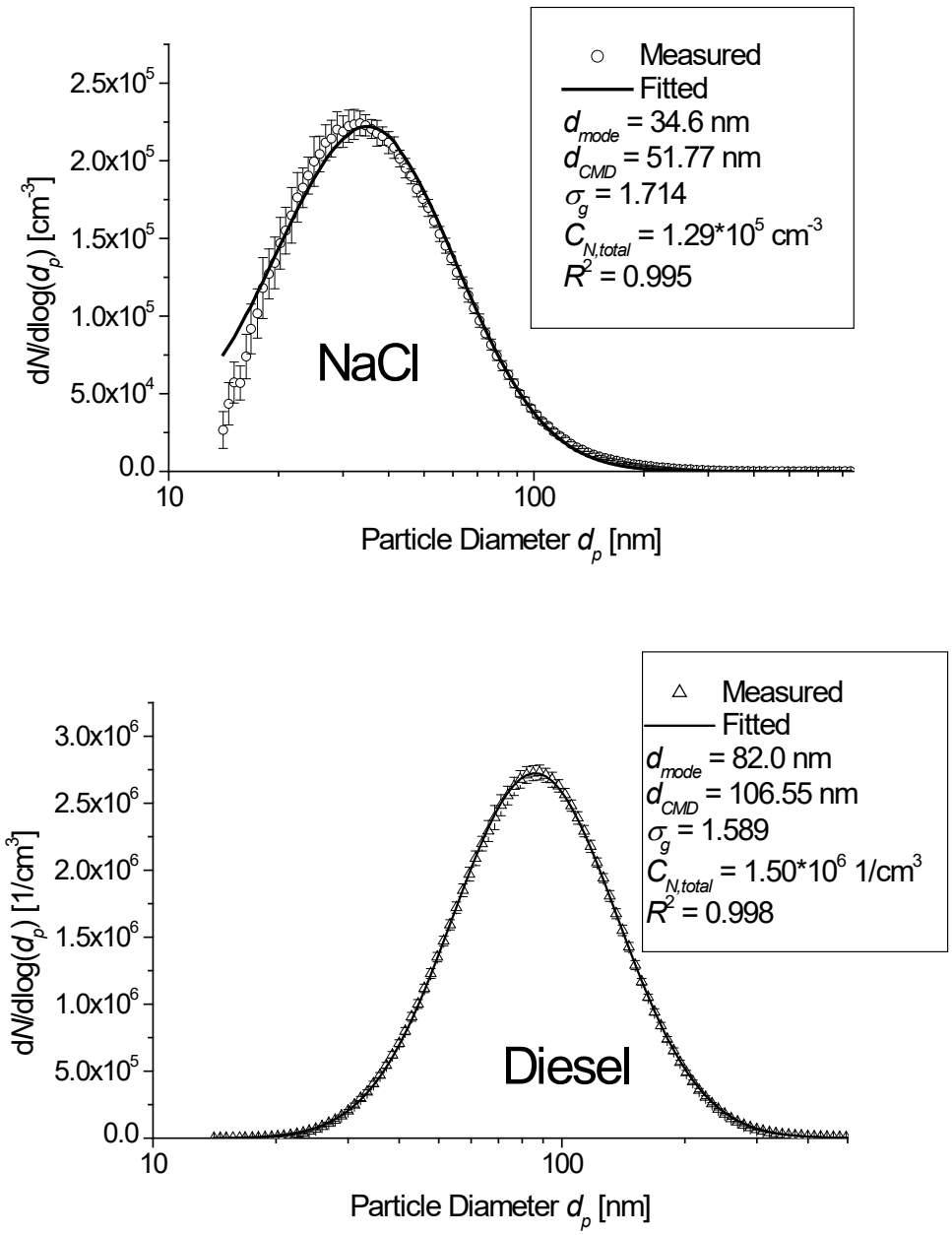
Measured
Fitted
d_{mode} = 34.6 nm
d_{CMD} = 51.77 nm
σ_g = 1.714
$C_{N,total}$ = 1.29*10^5 cm^{-3}
R^2 = 0.995
NaCl
dN/dlog(d_p) [cm^{-3}]
Particle Diameter d_p [nm]
Measured
Fitted
d_{mode} = 82.0 nm
d_{CMD} = 106.55 nm
σ_g = 1.589
$C_{N,total}$ = 1.50*10^6 1/cm^3
R^2 = 0.998
Diesel
dN/dlog(d_p) [1/cm^3]
Particle Diameter d_p [nm]

Figure 3

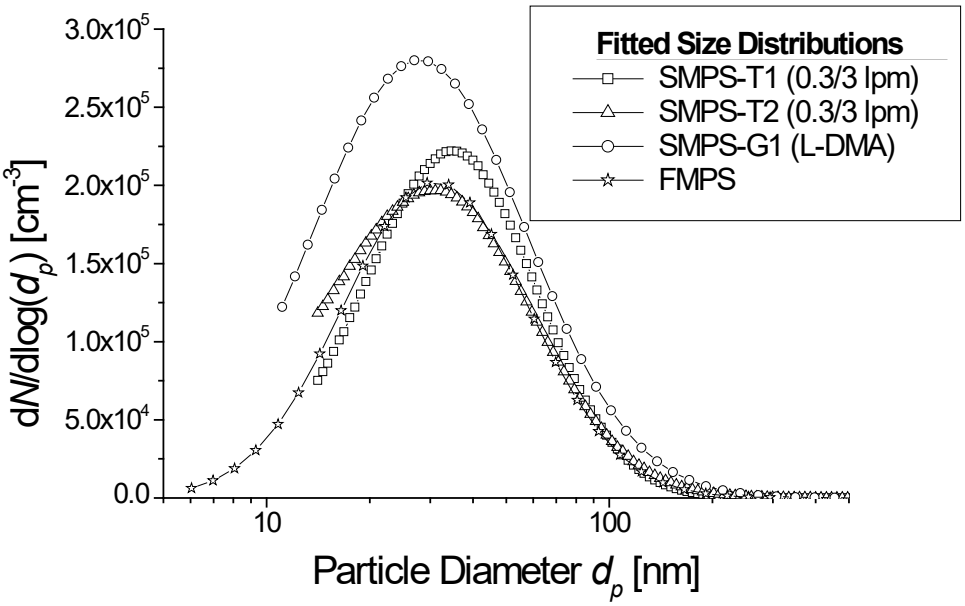
Fitted Size Distributions
SMPS-T1 (0.3/3 lpm)
SMPS-T2 (0.3/3 lpm)
SMPS-G1 (L-DMA)
FMPS
dN/dlog(d_p) [cm^-3]
3.0x10^5
2.5x10^5
2.0x10^5
1.5x10^5
1.0x10^5
5.0x10^4
0.0
10
100
Particle Diameter d_p [nm]

Figure 4

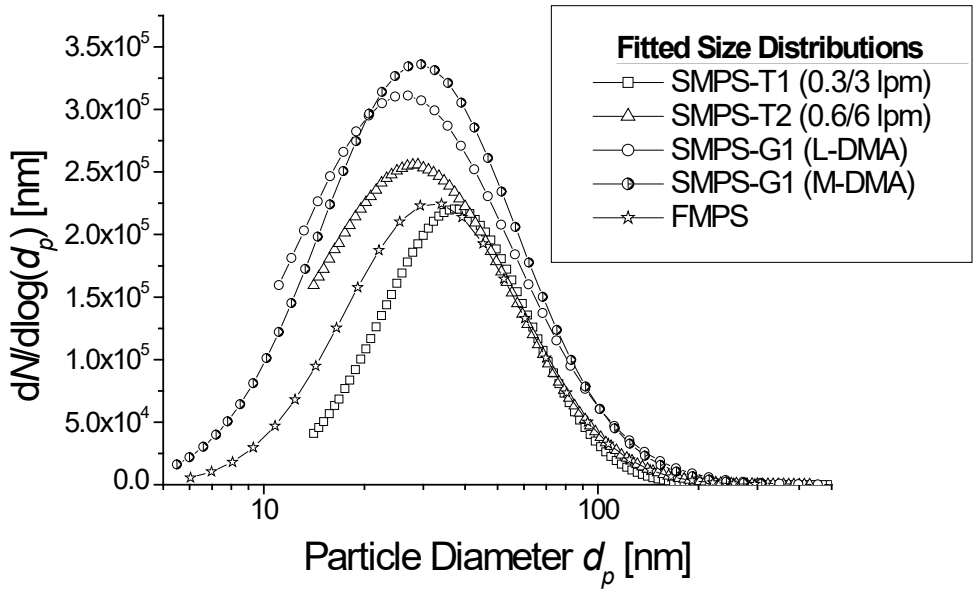
Fitted Size Distributions
SMPS-T1 (0.3/3 lpm)
SMPS-T2 (0.6/6 lpm)
SMPS-G1 (L-DMA)
SMPS-G1 (M-DMA)
FMPS
dN/dlog(d_p) [nm]
3.5x10^5
3.0x10^5
2.5x10^5
2.0x10^5
1.5x10^5
1.0x10^5
5.0x10^4
0.0
10
100
Particle Diameter d_p [nm]

Figure 5

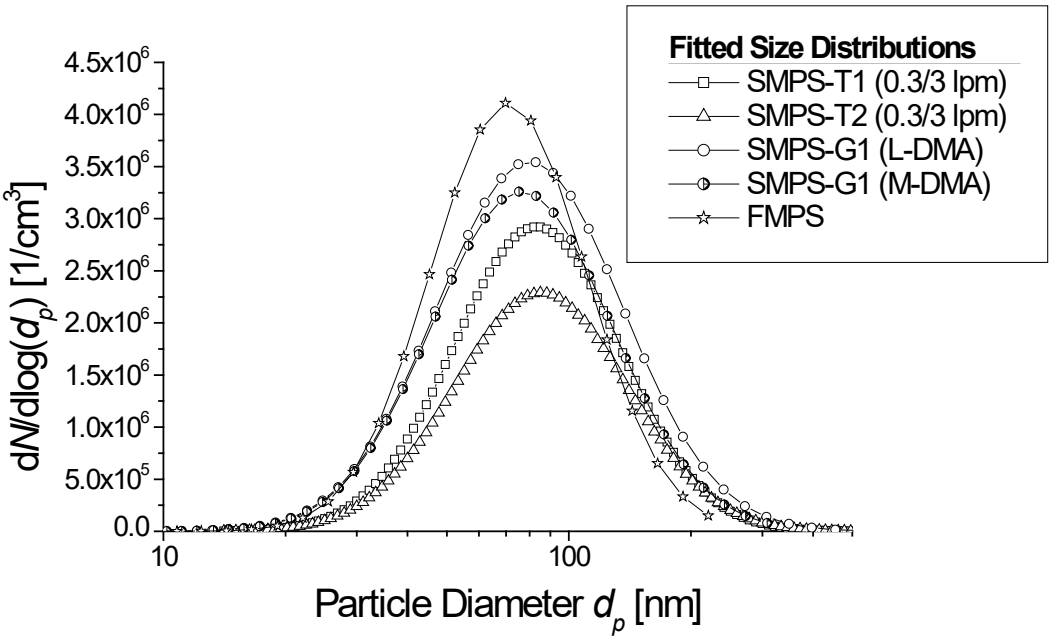
Fitted Size Distributions
SMPS-T1 (0.3/3 lpm)
SMPS-T2 (0.3/3 lpm)
SMPS-G1 (L-DMA)
SMPS-G1 (M-DMA)
FMPS
dN/dlog(d_p) [1/cm^3]
4.5x10^6
4.0x10^6
3.5x10^6
3.0x10^6
2.5x10^6
2.0x10^6
1.5x10^6
1.0x10^6
5.0x10^5
0.0
10
100
Particle Diameter d_p [nm]

Figure 6

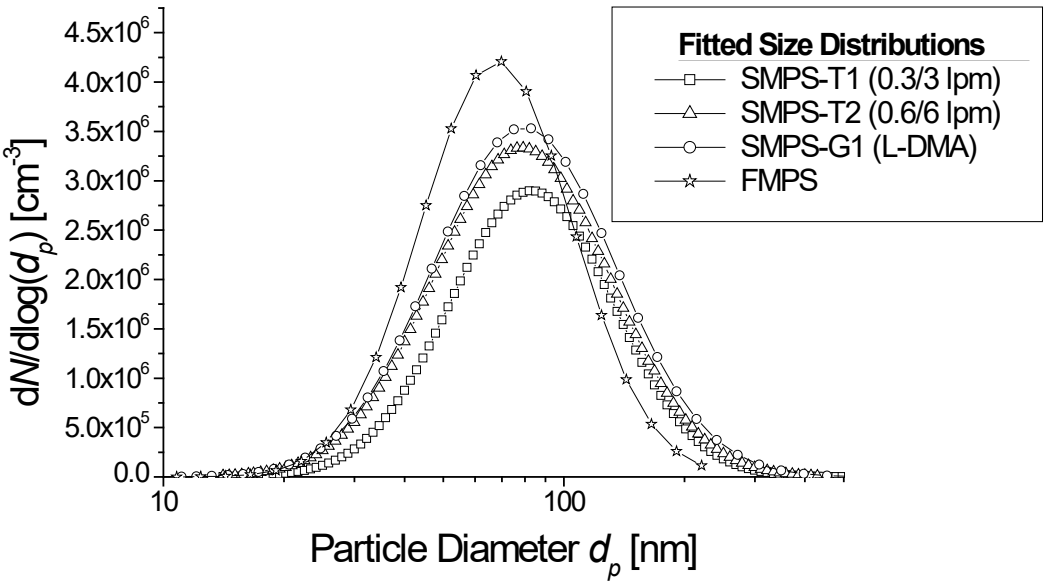
Fitted Size Distributions
SMPS-T1 (0.3/3 lpm)
SMPS-T2 (0.6/6 lpm)
SMPS-G1 (L-DMA)
FMPS
dN/dlog(d_p) [cm^-3]
4.5x10^6
4.0x10^6
3.5x10^6
3.0x10^6
2.5x10^6
2.0x10^6
1.5x10^6
1.0x10^6
5.0x10^5
0.0
10
100
Particle Diameter d_p [nm]

Figure 7

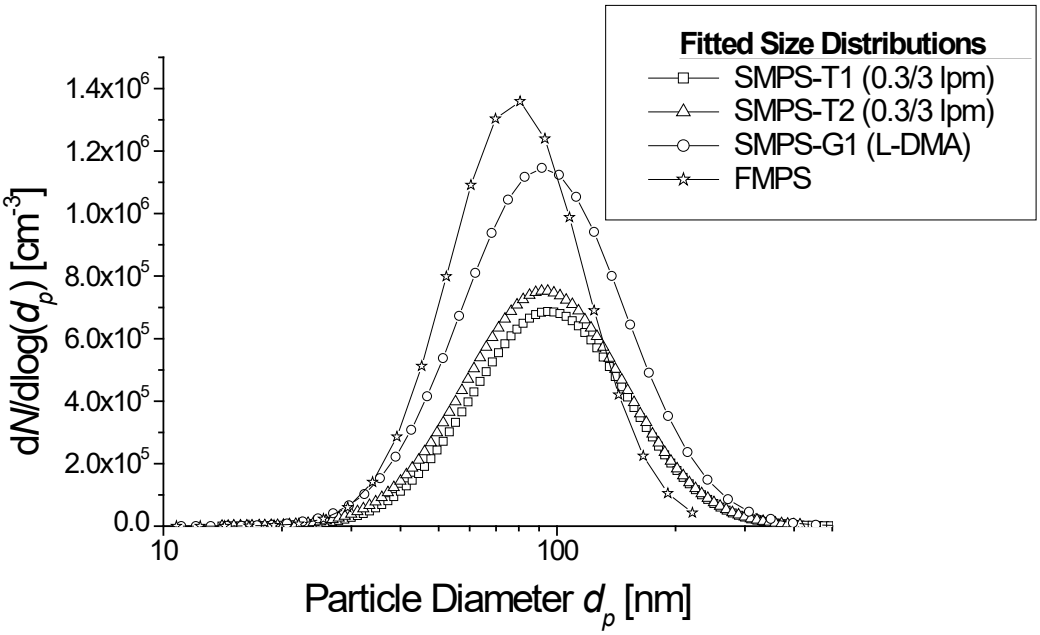
Fitted Size Distributions
SMPS-T1 (0.3/3 lpm)
SMPS-T2 (0.3/3 lpm)
SMPS-G1 (L-DMA)
FMPS
dN/dlog(d_p) [cm^-3]
1.4x10^6
1.2x10^6
1.0x10^6
8.0x10^5
6.0x10^5
4.0x10^5
2.0x10^5
0.0
10
100
Particle Diameter d_p [nm]

Table 1

	ID	Manufacturer/Model	Flow Rate Settings	Other Settings	Diameter Range	Particle Counter
SMPS	SMPS-T1	TSI/3080	0.3 lpm aerosol, 3 lpm sheath (always)	long DMA (always)	13.8 - 749.9 nm	TSI Water CPC, Model 3786
	SMPS-T2	TSI/3080	0.3 lpm aerosol, 3 lpm sheath	long DMA (always)	13.8 - 749.9 nm	TSI UCPC, Model 3010
			0.6 lpm aerosol, 6 lpm sheath	long DMA (always)	9.3 - 437.1 nm	TSI UCPC, Model 3010
	SMPS-G1	Grimm/SMPS+C	0.3 lpm aerosol, 3 lpm sheath (always)	M-DMA	5.5 - 350.4 nm	Grimm CPC, Model 5.404
				L-DMA	11.1 - 1083.3 nm	Grimm CPC, Model 5.404
FMPS	FMPS	TSI/3091	10 lpm aerosol, 40 lpm sheath (always)		5.6 - 562.3 nm	arrays of 22 electrometers
CPC	CPC-T1	TSI/3007	0.7 lpm total flow (always)		10 - 1000 nm	handheld
	CPC-T2	TSI/3007	0.7 lpm total flow (always)		10 - 1000 nm	handheld

Table 2

	Device ID	Setting	R^2	d_{mode} [nm]	d_{CMD} [nm]	σ_g	$C_{N,total}$ [1/cm³]
NaCl - 1st measurement	SMPS-T1	0.3/3 l/min	0.995	34.6	51.77	1.714	1.29e5
	SMPS-T2	0.3/3 l/min	0.990	32.2	52.45	1.852	1.28e5
	SMPS-G1	long DMA	0.998	29.4	46.68	1.860	1.83e5
	FMPS	default	0.963	27.0	45.77	2.047	1.36e5
	CPC-T1	default	--	--	--	--	9.43e4
	CPC-T2	default	--	--	--	--	1.03e5
NaCl - 2nd measurement	SMPS-T1	0.3/3 l/min	0.998	37.2	51.49	1.626	1.19e5
	SMPS-T2	0.6/6 l/min	0.999	28.9	48.91	1.853	1.59e5
	SMPS-G1	long DMA	0.998	27.0	45.78	2.107	2.03e5
	SMPS-G1	short DMA	0.998	29.6	45.77	1.964	2.13e5
	FMPS	default	0.964	34.0	46.84	1.849	1.38e5
	CPC-T1	default	--	--	--	--	1.01e5
	CPC-T2	default	--	--	--	--	1.09e5

Table 3

	Device ID	Setting	R^2	d_{mode} [nm]	d_{CMD} [nm]	σ_g	$C_{N,total}$ [1/cm³]
Diesel - 1st meas.	SMPS-T1	0.3/3 l/min	0.998	82.0	106.6	1.589	1.50e6
	SMPS-T2	0.3/3 l/min	1.000	85.1	110.9	1.614	1.22e6
	SMPS-G1	long DMA	0.997	82.8	105.7	1.694	2.03e6
	SMPS-G1	short DMA	0.995	75.4	99.2	1.666	1.81e6
	FMPS	default	0.995	69.8	86.1	1.556	1.98e6
Diesel - 2nd meas.	SMPS-T1	0.3/3 l/min	0.998	82.0	105.9	1.585	1.48e6
	SMPS-T2	0.6/6 l/min	0.999	79.1	103.9	1,638	1.84e6
	SMPS-G1	long DMA	0.998	82.8	104.6	1.686	2.01e6
	FMPS	default	0.990	69.8	82.3	1.550	2.01e6
Diesel - 3rd meas.	SMPS-T1	0.3/3 l/min	0.994	94.7	119.5	1.563	3.4e5
	SMPS-T2	0.3/3 l/min	1.000	91.4	117.3	1.574	3.79e5
	SMPS-G1	long DMA	0.997	91.5	115.5	1.609	5.93e5
	FMPS	default	0.991	80.6	91.6	1.481	5.82e5